

Molecular Design of β -Hairpin Peptides for Material Construction

Ronak V. Rughani and Joel P. Schneider

Abstract

Self-assembled materials composed of β -sheet forming peptides hold promise as therapeutics and novel biomaterials. This article focuses on the design and engineering of amphiphilic peptide sequences, especially β -hairpins. Peptides can be designed to intramolecularly fold and then self-assemble on cue, affording hydrogels rich in β -sheet structure. Hydrogels having distinct material properties can be designed at the molecular level by modulating either the peptide's sequence or the environmental stimulus used to trigger folding and assembly, leading to gelation.

Introduction

Proteins have evolved to fold, and in some cases self-assemble, into a vast array of beautiful structures, in large part to facilitate function. Their smaller cousins, peptides, are attractive building blocks for the construction of functional self-assembled materials owing to their smaller sequence length, ease of synthesis and purification, and a continuing advancement in the understanding of their folding and assembly propensities. The organization of peptides into ordered structures is guided by the formation of interactions such as hydrogen bonds, electrostatic interactions, hydrophobic contacts, and aromatic interactions.¹ The amide-containing backbone of peptides can facilitate the formation of H-bonds; amino acids that contain polar side chains can participate in the formation of electrostatic interactions such as salt bridges; cysteine residues can form disulfide linkages; histidine, tryptophan, phenylalanine, and tyrosine side chains can promote aromatic interactions; and hydrophobic side chains can facilitate van der Waals contact formation. Even extremely small peptides (<3 residues) can assemble into impressive structures using a combination of these interactions.²⁻⁴

A straightforward design strategy that can be used to construct peptides

capable of self-assembling into a large number of structures is to simply segregate amino acids along the peptide backbone with respect to their propensity to engage in a particular interaction. For example, amphiphilic peptides contain both hydrophobic and hydrophilic side chains that are segregated from each other. In the simplest of examples, segregation comes in two flavors. First, hydrophilic (A) and hydrophobic (B) residues can be segregated spatially along the length of the peptide sequence ($-[A]_n-[B]_n-$), resulting in diblock amphiphiles (Figure 1a). In a slightly more complex arrangement, residues are segregated spatially with respect to distinct faces of a folded peptide structure (Figure 1b). For example, a sequence of alternating hydrophilic and hydrophobic residues ($-[ABABAB]_n-$)⁵, which adopts an extended (linear) conformation, would have opposing hydrophilic and hydrophobic faces. Peptides having sequences such as ($-[BAABBAA]_n-$)⁶ can adopt facially amphiphilic helical structures that assemble into helical bundles. In aqueous solution, irrespective of the type of segregation, peptide assembly is largely driven by the desolvation (the release of ordered water around hydrophobes) and self-association of the

hydrophobic portions of the peptide; the self-association of hydrophobes is normally nonspecific with respect to the structural outcome of the self-assembly event. However, hydrophilic moieties can be used to design specific polar interactions that can help dictate the formation of a given structure over possible alternatives.

Although the following is not a comprehensive list, common structures resulting from the self-assembly of diblock amphiphiles include micelles,^{7,8} vesicles,⁹ and vesicular nanofibers¹⁰ (Figure 1a). Facial amphiphiles such as β -strands and β -hairpins often form fibrillar bilayers^{11,12} and higher-order laminates,^{13,14} extended fibrils, and extended β -sheets (Figure 1b).¹⁵ In addition, linear and cyclic peptides have been designed to assemble into tubes,^{16,17} and other peptides have been designed to assemble at surfaces.¹⁸⁻²⁰ Helical facial amphiphiles typically form discrete helical bundles or extended bundles^{21,22} (Figure 1b).

De Novo Designed Self-Assembling β -Hairpins

Schneider and Pochan have designed peptides that, in response to distinct external stimuli, fold into facially amphiphilic β -hairpins and subsequently self-assemble to form self-supporting, rigid hydrogels.^{11,23} β refers to the dihedral angle that defines the secondary structure of the peptide. The assembling mechanism allows material formation to take place with temporal resolution. The parent sequence, MAX1, is a 20-amino-acid peptide comprised of two β -strands with alternating valine and lysine residues. These amino acids have high β -sheet propensity. The strands are connected by a tetrapeptide ($-V^DPPPT-$) sequence designed to adopt a type II' turn structure (Figure 2b).¹¹ Under acidic conditions, the protonated lysines prevent the peptide from folding and thus self-assembling. However, intramolecular folding and consequent self-assembly can be triggered by either neutralizing the charge by increasing the pH of low-ionic-strength solutions to 9 or by screening the positively charged lysines by the addition of salt at physiological pH.^{11,23} Folding is largely governed by the electrostatic interactions of the hydrophilic face of the hairpin, the formation of intramolecular van der Waals contacts between side chains, and formation of intramolecular H-bonds between carbonyl and amide moieties of the peptide backbone (Figure 3a). In the folded state, amphiphilic MAX1 hairpins, where one face of the hairpin is valine-rich and the other lysine-rich, undergo both

facial and lateral association. Facial association occurs when the hydrophobic faces of the self-assembling hairpins collapse to form a bilayer-like structure. Lateral association occurs via the formation of intermolecular H-bonds and side chain-side chain hydrophobic contacts between assembling hairpins (Figure 3b). Self-

assembly via these mechanisms results in the formation of a non-covalently cross-linked network of short fibrils rich in β -sheet structure, resulting in mechanically rigid hydrogel (Figure 2a).

Structural characterization using transmission electron microscopy and small-angle neutron scattering²⁴ indicates that the

gel is composed of monodispersed fibrils with an average width of ~ 3 nm. This value corresponds to the width of the folded β -hairpin in the self-assembled state and provides support for the proposed self-assembly mechanism (Figure 2a). Fibrils are physically cross-linked by interfibril junctions and simple entanglements of fibrils. In the self-assembled state, fibrils are composed of a bilayer of intermolecularly hydrogen-bonded hairpins directed by the ordered packing of hydrophobic faces of individual hairpins. However, because of the topologically smooth surface of the hydrophobic face of each hairpin, facial mispacking occurs. This provides nucleation sites for nascent fibril growth in different three-dimensional directions creating branched junctions (Figure 2a). In addition to these interfibril junctions, fibrils can also become entangled. This provides additional physical cross-links. The number of fibril junctions and entanglements formed during the self-assembly process affects the mechanical rigidity of the hydrogels. When the kinetics of self-assembly is increased, more cross-links are formed and the resulting gels are more mechanically rigid. Conversely, slow self-assembly kinetics affords less rigid gels with fewer cross-links. For example, since the rate of self-assembly is concentration-dependent,²⁵ peptide concentration can be

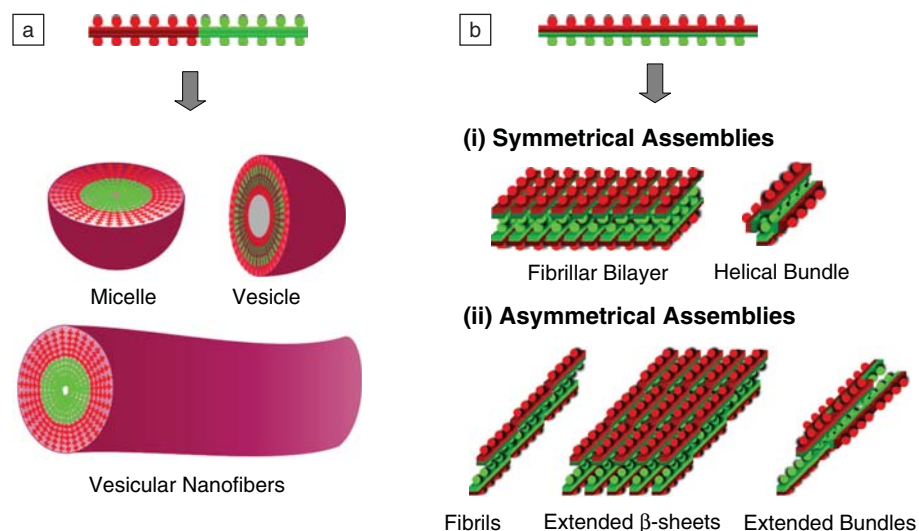


Figure 1. Self-assembled structures derived from peptide amphiphiles (red: hydrophilic, green: hydrophobic). (a) Diblock amphiphile, (b) facial amphiphile.

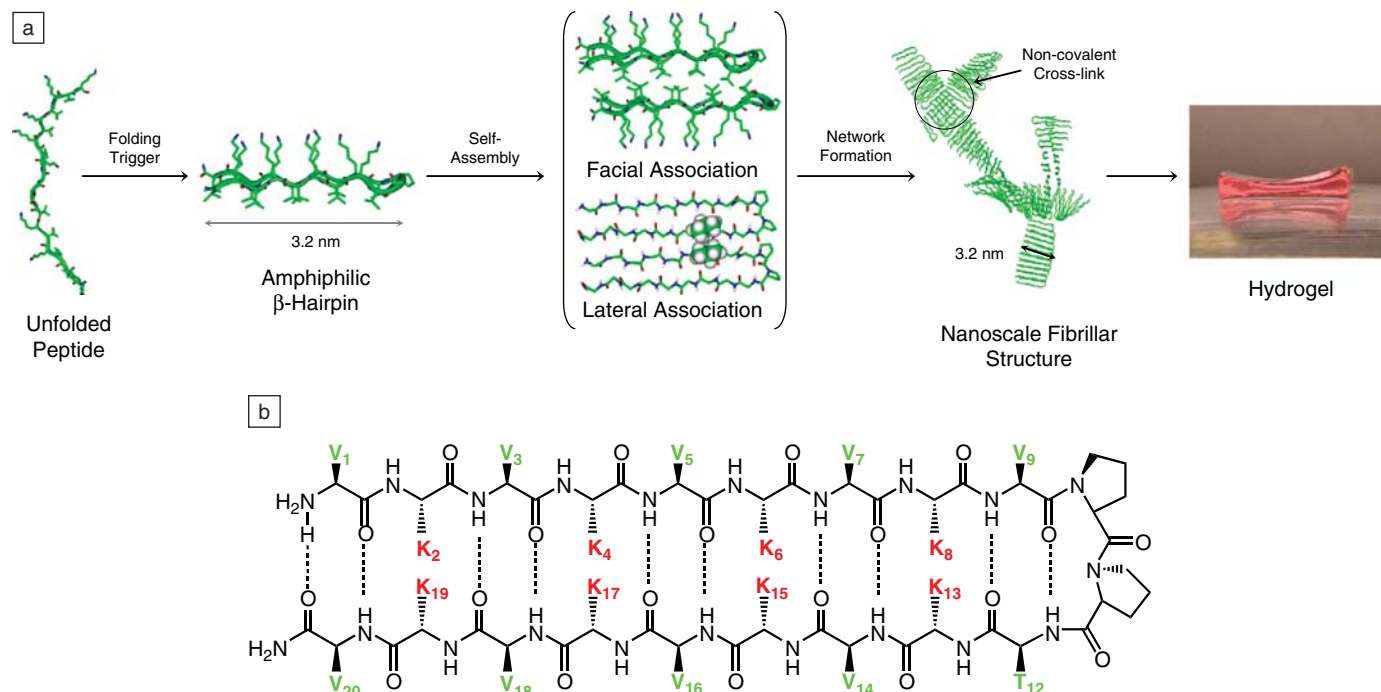


Figure 2. (a) Environmentally triggered folding, self-assembly, and non-covalent fibril cross-linking leading to hydrogelation. (b) β -hairpin structure of MAX1 comprised of two β -strands of alternating valine (green) and lysine (red) residues connected via a type II' β -turn.

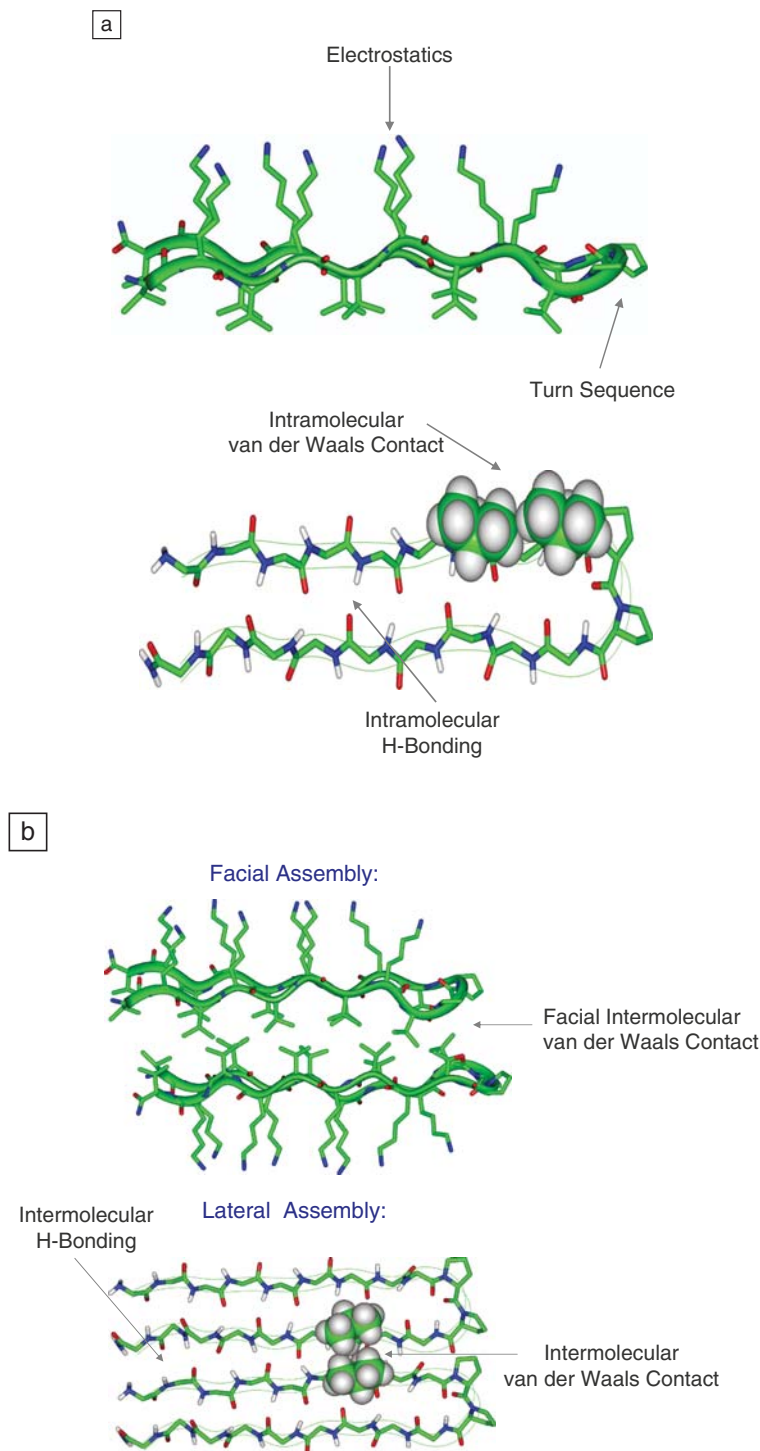


Figure 3. Factors affecting (a) folding and (b) self-assembly of β -hairpin peptides.

varied to modulate the kinetics of self-assembly and the ultimate mechanical rigidity of the resulting hydrogel.

In addition to altering the kinetics of self-assembly of MAX1 to prepare gels of

differing mechanical properties, we can also alter the amino-acid sequence. For example, each of the factors (outlined in Figure 3) that influence hairpin folding and self-assembly can be modulated by

amino-acid substitutions to fine-tune the mechanical properties of the gels.

Amino-Acid Substitutions at the Hydrophilic Face

Under acidic conditions, the lysine side chains in MAX1 are protonated, which prevents the peptide from folding and thus self-assembling. Unfolded MAX1 is highly soluble; solutions up to ~4wt% display rheological properties similar to water. Intramolecular folding and self-assembly is triggered by relieving the charge-charge repulsions with an increase in the pH or screening the charged lysines with the addition of salt at physiological conditions.^{11,23} In addition, peptide folding and self-assembly is reversible by altering the pH. This promotes deprotonation and reprotonation of the lysine side chains in low ionic salt solutions.¹¹ Since folding and self-assembly of MAX1 is dependent upon decreasing the electrostatic repulsions of the lysine side chains, reducing the charge density on the hydrophilic face by amino-acid substitution results in faster folding and self-assembly kinetics at pH 9. More importantly, lowering the positive-charge density on the hydrophilic face allows gelation at lower pH values. This is relevant for cell-based applications. For example, replacing the lysine at position 15 in MAX1 with glutamic acid (K15E) lowers the overall charge state by 2. At pH 7.4, the overall charge of MAX1 is +9 from eight lysine residues and one terminal amine whereas the overall charge of the K15E peptide is +7 (Figure 4). The resultant peptide, MAX8 (K15E), forms more rigid hydrogels than MAX1 at pH 7.4 with faster gelation kinetics.²⁶ In addition, this amino-acid substitution has little effect on the nanoscale morphology of the fibrils formed. Both gels, MAX1 and MAX8, showed an average fibril width of ~3 nm.²⁶ This was important to assess because peptides of similar secondary structure but differing in amino-acid composition and sequence have been reported to assemble into morphologically distinct structures such as laminating fibrils,^{1,27} ribbons and tapes,¹³ and tubes.^{9,17} Each morphology has distinct bulk-material properties. Comprehensive study of MAX8 gels suggests that rational modification of the net charge on the hydrophilic face can be used to control hydrogelation kinetics and thus the mechanical properties of the gel.²⁶

Amino-Acid Substitution at the Hydrophobic Face

MAX1 also undergoes heat-induced hydrogelation. At temperatures below ~20°C under low ionic strength solution conditions, MAX1 remains unfolded. When

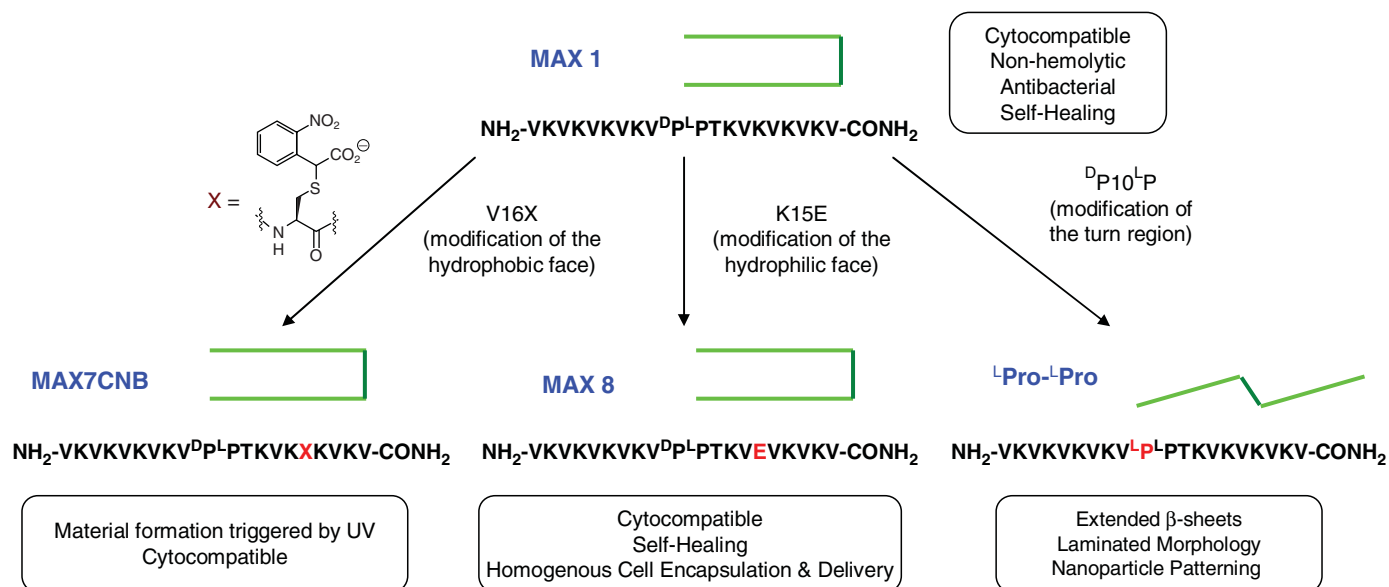


Figure 4. Structure-based design of MAX1. Modifications to the hydrophilic, hydrophobic, and turn regions to create new peptides with tailored properties.

the temperature increases, hydrophobic side chains are desolvated, and the peptide folds and self-assembles to bury its hydrophobic surfaces away from the water. Modulation of the hydrophobic character of the amphiphilic β -hairpin can be employed to control the temperature at which peptide folding and self-assembly is triggered. For example, valines were substituted with threonine to afford modified MAX1 variants: MAX2 (V16T) and MAX3 (V16T, V7T).²⁸ Threonine is isostructural with valine but less hydrophobic, therefore reducing the overall hydrophobicity of the valine-rich face. The exact temperature at which folding and self-assembly was triggered (T_{gel}) increased with a decrease in hydrophobic character of the amphiphilic peptide (MAX3 > MAX2 > MAX1). Interestingly, MAX3 exhibited thermoreversible self-assembly, affording a gel with properties that were highly influenced by environmental temperature. Circular dichroism and oscillatory rheology indicate that MAX3 remains unfolded and that its solution is of low viscosity at low temperatures (5°C) but folds and self-assembles at higher temperatures (75°C) to form a rigid self-supporting hydrogel. Subsequent temperature cycles showed that the conformational change and phase transitions were completely reversible. This indicated that formation of intra- and intermolecular hydrophobic interactions between the valine residues of MAX1 and MAX2 is a key factor in promoting folding and self-assembly to form physical irreversible cross-linked networks (Figure 3b).²⁸

Furthermore, Haines et al. incorporated a charged residue on the hydrophobic face, which disrupted hydrophobic interactions and thus inhibited folding and self-assembly of the β -hairpin peptide.²⁹ Incorporating charged residue(s) in a sequence to prevent self-assembly/aggregation is referred to as “negative design” or “gate keeping.” This has been found in naturally occurring proteins such as the S6 protein from *Thermus thermophilus*. Replacement of the gate-keeping charged residues with hydrophobic residues affords a mutant S6-Alz, which is capable of self-assembling into a tetramer.³⁰ To take advantage of this “negative design” concept, MAX7CNB was designed by the following method: a cysteine with a negatively charged photosensitive group on its side chain was substituted for a valine in MAX1 (Figure 4). As expected, this charged bulky residue inhibited the folding and self-assembly process. However, upon photocleavage, a moderately hydrophobic thiol is generated. This allows folding and self-assembly to proceed, affording a rigid hydrogel. This novel design affords a peptide whose hydrogelation can be triggered upon ultraviolet illumination.²⁹

Importance of Hydrogen Bonding and Hydrophobic (van der Waals) Contacts

In addition to hydrophobic and electrostatic interactions, peptide self-assembly is also directed by the formation of a network of H-bonds (between the amide NH

and C=O moieties). A common technique employed to analyze the formation of hydrogen bonds in self-assembled β -sheet networks is Fourier transform infrared spectroscopy (FTIR). The amide I band arising primarily from the backbone carbonyl stretch mode is sensitive to peptide secondary structure.³¹ In the case of a self-assembling β -hairpin, under unfolded conditions, the peptide in random-coil conformation displays a broad amide I band centered around 1644 cm^{-1} . Following folding and self-assembly, the amide I band shifts to form a well-defined peak at 1615 cm^{-1} . This strongly suggests formation of a self-assembled β -sheet rich structure.^{11,32} A weaker band of 1680 cm^{-1} is also observed and is often associated with an antiparallel β -sheet arrangement.³³ According to our proposed mechanism, MAX1 would be expected to fold into a symmetrical β -hairpin where all of the intramolecular H-bond donors (NH) and acceptors (C=O) are satisfied. However, monomeric hairpins contain unfulfilled acceptors and donors at the β -strand edges. These acceptors and donors can participate in intermolecular H-bond formation with other hairpins during self-assembly. Ultimately, folding and self-assembly result in the formation of a network of intra- and intermolecular H-bonds along the long axis of fibrils that constitute the gel. We have found that disrupting the ability of peptides to form symmetrical intra- and intermolecular H-bonds grossly influences fibril nanostructure and consequent hydrogel mechanical properties.⁴⁵

Additional studies indicate that lateral self-assembly is also governed by intermolecular hydrophobic contacts between the residue side chains of neighboring hairpins (Figure 3). In MAX1, the valine residues are placed at H-bonding positions and lysines are placed at the non-H-bonding positions within the primary sequence of each strand. According to Wouters and Curmi,³⁴ valine residues prefer to adopt a *trans* χ_1 side-chain rotamer when contained within β -sheet structures. Therefore, a large portion of MAX1 valine side chains should adopt *trans* dihedral angles, directing their isopropyl side chains away from the center of the hairpin and extending them toward the valine side chains of neighboring hairpins. Thus, the formation of valine-based lateral hydrophobic contacts should drive self-assembly and contribute to the rigidity of the hydrogel. This was confirmed with an inverse design of MAX1.³⁵ This peptide, MAX4, has the same number of residues and a similar turn region as MAX1 but contains β -strand sequences with valine residues at non-H-bonded positions and lysine residues at H-bonded positions (the exact opposite of MAX1). MAX4 should be largely incapable of forming valine-derived lateral intermolecular contacts. In fact, MAX4 not only exhibited slower kinetics of folding and self-assembly but also formed a less rigid hydrogel than MAX1. In addition, structural characterization of MAX4 revealed formation of higher-order assemblies unlike MAX1.³⁵ This indicated that valines at H-bonded positions are also important to achieving well-defined fibril morphology and a mechanically rigid hydrogel.

Importance of Turn-Region Residues

Turn regions in proteins and peptides are an important class of structures that strongly influence both structure and function. One such turn type is the β or reverse turn. In this case, the turn causes the polypeptide chain to reverse direction after the location of the turn in the peptide sequence.³⁶ A β -turn is typically composed of a four-residue sequence (denoted as the i to $i+3$ residues) that connects two secondary structural elements and may play a significant role in initiating folding and in stabilizing tertiary structures. Different types of β -turns have been identified and classified according to the main-chain dihedral angles (Φ, Ψ) that their $i+1$ and $i+2$ residues adopt. Each turn type influences β -sheet properties such as β -sheet twist, stability, folding nucleation rate, and the hydrogen-bonding registry.³⁷ Systematic studies indicate that β -turn type and the

propensity of the residues occupying turn positions to adopt dihedral angles consistent with β -turn structure influence the formation and stability of β -hairpins.^{38–40} MAX1 contains a tetrapeptide sequence ($-V^D P^L P^L P^T-$) that has high propensity to adopt a type II' β -turn due, in part, to the chirality of the D prolyl residue at the $i+1$ position (Figure 2). Valine, a β -branched residue, at the i position (V_i) of the turn, enforces a *trans*-prolyl amide bond geometry at the succeeding ($i+1$) position. A threonine residue at the $i+3$ position of the turn region has a high propensity to occupy this position in type II' turns of hairpins of naturally occurring proteins.⁴¹ Threonine can form a stabilizing side-chain-main-chain H-bond between its alcoholic proton and the carbonyl oxygen of the i th residue of the turn. A control peptide [(VK)₄] (i.e., without the turn region), under folding conditions (pH 9.0), failed to form a hydrogel at ambient temperature. This demonstrates that the turn region is necessary for the folding and self-assembly of MAX1 leading to hydrogelation.¹¹

In addition, the stereochemistry of the turn residues is also important in directing the self-assembly process. Lamm et al. investigated this by replacing the D proline at the $i+1$ position in the turn with the stereoisomer and naturally occurring amino acid L proline ($-V^L P^L P^L P^T-$). This peptide (L P^LP) was unable to intramolecularly fold but was still capable of self-assembly into a β -sheet rich structure.³² Unlike MAX1 that folds into a β -hairpin and subsequently self-assembles to form monodispersed well-defined fibrils,^{23,24} L P^LP adopts an extended β -strand conformation (Figure 4) and assembles into H-bonded fibrils exhibiting a highly laminated, non-twisted morphology.³²

Functional Materials From Self-Assembling β -Hairpins Mimics of Extracellular Matrix

When fabricating hydrogels for tissue-engineering applications such as soft-tissue regeneration⁴⁶ or cell delivery,²⁶ several general material and biological requirements have to be considered. The scaffold should be self-supporting and mechanically rigid in the presence of cells, porous enough to allow diffusion of nutrients and waste, cytocompatible, and biocompatible. Cytocompatible scaffolds are nontoxic to cells and support cell adhesion and proliferation events. Rheological measurements indicated that MAX1 forms mechanically rigid hydrogels on addition of cell-culture media (DMEM). MAX1 hydrogel surfaces not only proved to be nontoxic to NIH 3T3 fibroblasts (commercially available cells that produce

collagen and other fibers) but also allowed facile cell attachment both in the presence and absence of serum. In addition, cells can proliferate on the gel surface with minimal effect on the rheological properties of the scaffold.⁴² MAX8 is also cytocompatible with a broad range of mammalian cells including fibroblasts, stem cells, chondrocytes, and pre-osteoblasts. In addition, MAX8's fast-assembly kinetics allows homogenous three-dimensional incorporation of cells when gelation is triggered in the presence of cells. Homogenous encapsulation is significant since cell density plays an important role in modulating the behavior of delivered cells.⁴³

Injectable Delivery

Both MAX1 and MAX8 hydrogels shear thin when a significant stress is applied to the material. However, when the application of shear stress is stopped, the gels immediately self-heal. This shear thinning/self-healing behavior allows for delivery of the gels through syringes to targeted sites. Depressing the syringe barrel provides sufficient shear stress to convert the mechanically rigid gel into a viscous gel that flows. After the flowing gel leaves the tip of the needle, it immediately recovers, forming a gel with near quantitative recovery of its original storage modulus. When MAX8 gels are impregnated with cells, this mechanism can be used to deliver cells to wound sites with spatial resolution. Cells remain viable during encapsulation and the shear-thin delivery process, and gel-cell constructs stay localized at the site of introduction. These properties make the gels useful for delivery of cells to targeted biological sites in tissue-regeneration efforts.²⁶

Antibacterial Activity

Among several important considerations for implantation of a biomaterial, a main concern is the introduction of infection. The surfaces of MAX1 hydrogels exhibit inherent antibacterial activity. In experiments, MAX1 hydrogel surfaces were challenged with bacterial solutions ranging in concentrations from 2×10^3 colony-forming units (CFUs)/dm² to 2×10^9 CFUs/dm² to demonstrate its broad-spectrum antibacterial activity.⁴⁴ Results showed that the hydrogel surface was active against Gram-positive (*Staphylococcus epidermidis*, *Staphylococcus aureus*, and *Streptococcus pyogenes*) and Gram-negative (*Klebsiella pneumoniae* and *Escherichia coli* (*E. coli*)) bacteria, all prevalent in hospital settings. Live-dead assays employing laser scanning confocal microscopy showed that bacteria die

when they engage the surface. In addition, enzyme-based assays indicated that the surfaces of MAX1 hydrogels cause the disruption of the inner and outer membranes of *E. coli*. This data suggested a mechanism of antibacterial action that involved membrane disruption leading to cell death upon cellular contact with the gel surface. Although the hydrogel surface exhibited bactericidal activity, co-culture experiments indicated that the hydrogel surfaces show selective toxicity to bacterial versus mammalian cells. Additionally, gel surfaces were nonhemolytic toward human erythrocytes, which maintained healthy morphologies when in contact with the surface. These material attributes make MAX1 gels attractive candidates for use in tissue regeneration, even in non-sterile environments.⁴⁴

Conclusions

Peptide-based materials are showing potential for nanotechnological and biomedical applications. Continuing research is providing insight into the factors that direct the self-assembly process of peptides leading to targeted structures with specific functions. The discovery phase of this research is extremely exciting. However, in order to realize the full potential of these materials, a cost-effective synthetic or biological process will need to be developed to facilitate large-scale production of peptides for bulk use. In addition, peptide purity is sometimes overlooked in the literature but is very important to ensure batch-to-batch consistency in both material and biological properties. For biomedical applications, it is essential to assess the material's potential to illicit the immune response early on in a material's developmental stage. These studies are expensive and become cost-prohibitive for an academic lab generating libraries of material. Therefore, an *ex vivo* assay that pre-screens a material's potential to illicit the immune response would catalyze the bench-top to bedside process.

Acknowledgments

This work was supported in part by the National Institutes of Health National

Institute of Dental and Craniofacial Research Grant R01 DE01638601 and the National Science Foundation (CHEM 0348323).

References

1. K. Rajagopal, J.P. Schneider, *Curr. Opin. Struct. Biol.* **14**, 480 (2004).
2. Z. Yang, B. Xu, *J. Mater. Chem.* **17**, 2385 (2007).
3. E. Gazit, *Chem. Soc. Rev.* **36**, 1263 (2007).
4. R.J. Mart, R.D. Osborne, M.M. Stevens, R.V. Ulijn, *Soft Matter* **2**, 822 (2006).
5. A. Brack, L.E. Orgel, *Nature* **256**, 383 (1975).
6. D.P. Raleigh, S.F. Betz, W.F. DeGrado, *J. Am. Chem. Soc.* **117**, 7558 (1995).
7. T. Gore, Y. Dori, Y. Talmon, M. Tirrell, H. Bianco-Peled, *Langmuir* **17**, 5352 (2001).
8. T. Koga, M. Higuchi, T. Kinoshita, N. Higashi, *Chem. Eur. J.* **12**, 1360 (2006).
9. G. von Maltzahn, S. Vauthey, S. Santoso, S. Zhang, *Langmuir* **19**, 4332 (2003).
10. J.D. Hartgerink, E. Beniash, S.I. Stupp, *Proc. Natl. Acad. Sci. U.S.A.* **99**, 5133 (2002).
11. J.P. Schneider, D.J. Pochan, B. Ozbas, K. Rajagopal, L. Pakstis, J. Kretsinger, *J. Am. Chem. Soc.* **124**, 15030 (2002).
12. H. Dong, S.E. Paramonov, L. Aulisa, E.L. Bakota, J.D. Hartgerink, *J. Am. Chem. Soc.* **129**, 12468 (2007).
13. A. Aggeli, I.A. Nyrkova, M. Bell, R. Hardick, L. Carrick, T.C.B. McLeish, A.N. Semenov, N. Boden, *Proc. Natl. Acad. Sci. U.S.A.* **98**, 11857 (2001).
14. S. Ramachandran, J. Trehwella, Y. Tseng, Y.B. Yu, *Chem. Mater.* **18**, 6157 (2006).
15. H. Yokoi, T. Kinoshita, S. Zhang, *Proc. Natl. Acad. Sci. U.S.A.* **102**, 8414 (2005).
16. D.T. Bong, M.R. Ghadiri, *Angew. Chem. Int. Ed.* **40**, 2163 (2001).
17. K. Lu, J. Jacob, P. Thiyagarajan, V.P. Conticello, D.G. Lynn, *J. Am. Chem. Soc.* **125**, 6391 (2003).
18. E. Powers, S. Yang, C. Lieber, J. Kelly, *Angew. Chem. Int. Ed.* **41**, 127 (2002).
19. G. Xu, W. Wang, J.T. Groves, M.H. Hecht, *Proc. Natl. Acad. Sci. U.S.A.* **98**, 3652 (2001).
20. H. Rapaport, K. Kjaer, T.R. Jensen, L. Leiserowitz, D.A. Tirrell, *J. Am. Chem. Soc.* **122**, 12523 (2000).
21. D.N. Woolfson, *Fibrous Proteins: Coiled-Coils, Collagen and Elastomers* **70**, 79 (2005).
22. Y. Zimenkov, S.N. Dublin, R. Ni, R.S. Tu, V. Breedveld, R.P. Apkarian, V.P. Conticello, *J. Am. Chem. Soc.* **128**, 6770 (2006).
23. B. Ozbas, J. Kretsinger, K. Rajagopal, J.P. Schneider, D.J. Pochan, *Macromolecules* **37**, 7331 (2004).
24. B. Ozbas, K. Rajagopal, J.P. Schneider, D.J. Pochan, *Phys. Rev. Lett.* **93**, 268106 (2004).
25. C. Veerman, K. Rajagopal, C.S. Palla, D.J. Pochan, J.P. Schneider, E.M. Furst, *Macromolecules* **39**, 6608 (2006).
26. L. Haines-Butterick, K. Rajagopal, M. Branco, D. Salick, R. Rughani, M. Pilarz, M.S. Lamm, D.J. Pochan, J.P. Schneider, *Proc. Natl. Acad. Sci. U.S.A.* **104**, 7791 (2007).
27. M. Lopez de la Paz, K. Goldie, J. Zurdo, E. Lacroix, C.M. Dobson, A. Hoenger, L. Serrano, *Proc. Natl. Acad. Sci. U.S.A.* **99**, 16052 (2002).
28. D.J. Pochan, J.P. Schneider, J. Kretsinger, B. Ozbas, K. Rajagopal, L. Haines, *J. Am. Chem. Soc.* **125**, 11802 (2003).
29. L.A. Haines, K. Rajagopal, B. Ozbas, D.A. Salick, D.J. Pochan, J.P. Schneider, *J. Am. Chem. Soc.* **127**, 17025 (2005).
30. D. Thirumalai, D. Klimov, R. Dima, *Curr. Opin. Struct. Biol.* **13**, 146 (2003).
31. S.M. Decatur, *Acc. Chem. Res.* **39**, 169 (2006).
32. M.S. Lamm, K. Rajagopal, J.P. Schneider, D.J. Pochan, *J. Am. Chem. Soc.* **127**, 16692 (2005).
33. W.K. Surewicz, H.H. Mantsch, D. Chapman, *Biochemistry* **32**, 389 (1993).
34. M.A. Wouters, P.M.G. Curmi, *Protein Struct. Funct. Genet.* **22**, 119 (1995).
35. K. Rajagopal, B. Ozbas, D.J. Pochan, J.P. Schneider, *Eur. Biophys. J. Biophys. Lett.* **35**, 162 (2006).
36. I. Karle, H.N. Gopi, P. Balaram, *Proc. Natl. Acad. Sci. U.S.A.* **99**, 5160 (2002).
37. A.C. Gibbs, T.C. Bjorn Dahl, R.S. Hodges, D.S. Wishart, *J. Am. Chem. Soc.* **124**, 1203 (2002).
38. H.E. Stanger, S.H. Gellman, *J. Am. Chem. Soc.* **120**, 4236 (1998).
39. J.F. Espinosa, F.A. Syud, S.H. Gellman, *Protein Sci.* **11**, 1492 (2002).
40. E. de Alba, M. Rico, M.A. Jimenez, *Protein Sci.* **8**, 2234 (1999).
41. E.G. Hutchinson, J.M. Thornton, *Protein Sci.* **3**, 2207 (1994).
42. J.K. Kretsinger, L.A. Haines, B. Ozbas, D.J. Pochan, J.P. Schneider, *Biomaterials* **26**, 5177 (2005).
43. M. Dvir-Ginzberg, I. Gamieli-Bonshtein, R. Agbaria, S. Cohen, *Tissue Eng.* **9**, 757 (2003).
44. D.A. Salick, J.K. Kretsinger, D.J. Pochan, J.P. Schneider, *J. Am. Chem. Soc.* **129**, 14793 (2007).
45. R. P. Nagarkar, R. A. Hule, D. J. Pochan, J.P. Schneider, *J. Am. Chem. Soc.*, 2008 (10.1021/ja.710295t).
46. Tanyarut Boonthekul, Elliott E. Hill, Hyun-Joon Kong, David J. Mooney. *Tissue Engineering*. July 1, 2007, 13(7): 1431-1442. doi:10.1089/ten.2006.0356. □



MRS
materials360PLUS™
www.mrs.org/360plus

Materials News
Materials Information
Resources and Links
Meetings Calendar
and Much More!